RSC Advances

PAPER

View Article Online
View Journal | View Issue

Cite this: *RSC Adv.*, 2017, **7**, 678

Quantum size effect and catalytic activity of nanosized single-crystalline spherical β-Ga_2O_3 particles by thermal annealing of liquid metal nanoparticles†

Shinya Sudo,[a] Kenta Kokado*[ab] and Kazuki Sada*[ab]

Received 31st October 2016
Accepted 28th November 2016

DOI: 10.1039/c6ra26085c

www.rsc.org/advances

We report on the synthesis of nanosized single-crystalline spherical β-Ga_2O_3 particles (**GONP**) by thermal annealing of gallium nanoparticles (**GaNP**), which previously has been prepared under ultrasonication. **GONP** displayed a spherical morphology and the particle size reflected that of **GaNP**. The nanoparticles have been confirmed as crystalline β-Ga_2O_3 by powder X-ray diffraction. The selected area electron diffraction patterns obtained from a whole particle of one **GONP** represented production of single-crystalline nanoparticle. Furthermore, the dispersibility and stability of **GONP** in solvent dramatically improved through silica coating (**GO@SiO_2 NP**). Photoluminescence spectroscopy indicated that the **GO@SiO_2 NP** exhibited a light blue emission at 445 nm under excitation at 240 nm. Diffuse reflectance spectroscopy demonstrated that the band gap of **GO@SiO_2 NP** (E_g = 4.89 eV) was hypsochromically shifted compared to that of bulk Ga_2O_3 (E_g(bulk) = 4.56 eV) due to the quantum size effect of β-Ga_2O_3. Additionally, silica particle-supported **GONP** (**GONP/MCM-41**) showed catalytic activity for the benzylation of benzene with benzyl chloride. Thus, the **GONP** presented here will have potential applications in LED phosphors, optoelectronic devices, and supported catalysts.

Introduction

Monoclinic gallium oxide (β-Ga_2O_3) is a well-known wide-band-gap semiconductor (E_g > 4.4 eV) that exhibits luminescence and conduction properties.[1–4] Due to these unique performances, β-Ga_2O_3 can be used for a variety of applications including electronic and optoelectronic devices, such as high sensitivity gas sensors, and transparent conductors.[5–10] Up to now, micrometer/nanometer scaled single-crystalline β-Ga_2O_3 with varied morphology, for instance, rods, wires, tubes, plates have been synthesized and characterized.[11–19] However, examples of the preparation of single-crystalline spherical β-Ga_2O_3 particles has still remained very few. Recently, Tang *et al.* have reported a simple method to prepare submicrometer-sized spherical β-Ga_2O_3 particles with uniform diameters.[20] The β-Ga_2O_3 submicron particle was synthesized by heating molten gallium, and the resulting particles exhibited a broad emission spectrum with a maximum at 458 nm under 260 nm excitation, since various quantum size effects in electronic, optical, and/or magnetic properties, such as an increase in the band gap of a semiconducting material with a reduction of the size, are generally observed for other materials.[21–27] Downsizing of β-Ga_2O_3 submicron particle will also provide distinctive quantum size effect on these properties. Nevertheless, to the best of our knowledge, preparation of single-crystalline spherical β-Ga_2O_3 nanoparticles and the quantum size effect have been never reported yet.

These facts prompted us to explore the quantum size effect of β-Ga_2O_3 particles. We previously reported preparation of liquid-metal nanocolloid composed of liquid gallium, solvents, and surfactants with ultrasonic irradiation.[28] The direct synthesis method enabled to control the size of gallium nanoparticle (**GaNP**) by tuning the surfactants, temperature, and ultrasonic irradiation intensity.

In this report, we demonstrate for the first time preparation of single-crystalline spherical β-Ga_2O_3 nanoparticle (**GONP**) derived from **GaNP** as precursor (Fig. 1). To suppress the aggregation of prepared **GONP**, we selected silica coated **GaNP** (**Ga@SiO_2 NP**) as precursors of **GONP**. The obtained **GONP** exhibited luminescence property and hypsochromic shift of band gap due to quantum size effect of β-Ga_2O_3. Furthermore, the **GONP** were supported on MCM-41, resulting in catalytic activity for Friedel–Crafts type benzylation.

Experimental section

Materials and instrumentation

Gallium (high purity, 99.9999%, Mitsuwa Chemicals Co., Ltd.), dodecylamine (Tokyo Chemical Industry Co., Ltd.), oleic acid

[a]*Graduate School of Chemical Sciences and Engineering, Hokkaido University, Kita10 Nishi8, Kita-ku, Sapporo, Hokkaido, 060-0810, Japan. E-mail: kokado@sci.hokudai.ac.jp; sadatcm@mail.sci.hokudai.ac.jp*

[b]*Faculty of Science, Hokkaido University, Japan*

† Electronic supplementary information (ESI) available: Histogram of diameter, Brus equation, fluorescence and reflectance spectra. See DOI: 10.1039/c6ra26085c

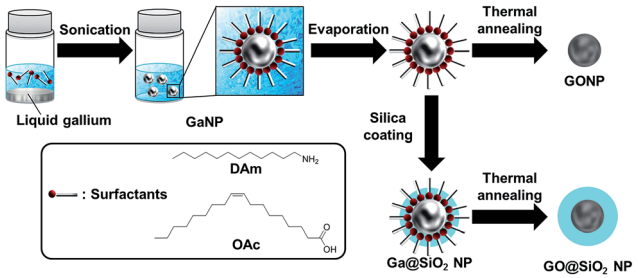

Fig. 1 Schematic illustration of preparation of spherical β-Ga_2O_3 nanoparticle (GONP) and silica-coated β-Ga_2O_3 nanoparticle (GO@SiO_2 NP) from gallium nanoparticle (GaNP) as precursors. Surfactants are dodecylamine (DAm) or oleic acid (OAc).

(Wako chemical industries, Ltd.), tetramethyl orthosilicate (Tokyo Chemical Industry Co., Ltd.), chloroform (Wako chemical industries, Ltd.), 2-propanol (Wako chemical industries, Ltd.) were purchased from each company, and used without further purification. Sonication was carried out with ELMA Elmasonic S30H and SND US-2KS (80 W for **GaNPs@DAm** and 120 W for **GaNPs@OAc**). Powder X-ray diffraction (XRD) patterns were obtained by Bruker AXS D8 ADVANCE. Transmission electron microscopy (TEM) was conducted on a JEOL JEM-2100F having EDX function and a JEOL JEM-2010 for selected-area electron diffraction (SAED). Emission spectra were obtained with SHIMADZU RF5300PC spectrofluorometer. UV-Vis spectra were recorded on a JASCO V-570 spectrophotometer. ^{1}H (500 MHz) NMR spectra were measured on a Bruker Biospin AVANCE DRX500 instrument, using 0.05% tetramethylsilane (TMS) as an internal standard. TEM observation was conducted at the OPEN FACILITY, Hokkaido University Sousei Hall.

Preparation of GaNP suspension[28]

Metallic gallium (100 mg, 1.4 mmol) was added to a chloroform solution (2.4 mL) of dodecylamine (276 μL), and the solution was heated at 80 °C for 15 min. After visual confirmation of gallium melting, the solution was sonicated by a bath type sonicator at 0 °C for 10 min, which resulted in dodecylamine stabilized **GaNP** (**GaNP@DAm**) suspension.

Preparation of GONP

GaNP@DAm suspension was separated by centrifugation, and the **GaNP@DAm** powder was obtained by drying. **GONP** was prepared by thermal annealing under air using electric furnace and oven at 500–900 °C under ambient atmosphere for 1 hour.

Preparation of SiO_2 coated GaNP (Ga@SiO_2 NP)

Metallic gallium (100 mg, 1.4 mmol) was added to a chloroform solution (2.4 mL) of oleic acid (381 μL), and the solution was heated at 80 °C for 15 min. After confirmation of melting gallium, the solution was sonicated by bath type sonicator at 0 °C for 10 min, which resulted in oleic acid stabilized **GaNP** (**GaNP@OAc**) suspension. **GaNP@OAc** suspension was separated by centrifugation, and the **GaNP@OAc** powder was obtained by drying. Then, the **GaNP@OAc** powder was added to 90 mL 2-propanol, 7.2 mL water, and 900 μL ammonia solution. Under continuous stirring, 0.9 mg of tetramethyl orthosilicate (TMOS) was added to the reaction mixture. The reaction was allowed to proceed for 1 hour at room temperature under continuous stirring, which resulted in silica coated **GaNP@OAc** (**Ga@SiO_2 NP**) suspension.

Preparation of silica coated GONP (GO@SiO_2 NP)

Ga@SiO_2 NP suspension was separated by centrifugation and **Ga@SiO_2 NP** powder were obtained by drying. Silica coated **GONP** (**GO@SiO_2 NP**) was prepared by thermal annealing using electric furnace and oven at 700 °C for 1 hour.

Preparation of MCM-41 supported GONP (GONP/MCM-41)

GONP supported on MCM-41 (**GONP/MCM-41**) was synthesized by evaporation to dryness. MCM-41 (20 mg) was dispersed in chloroform (6 mL). Then, **GaNP@OAc** powder (2 mg) was added to MCM-41 dispersion. After ultrasonication, the mixture was evaporated to dryness, which resulted in **GaNP@OAc** supported on MCM-41. Supported **GONP** was prepared from **GaNP@OAc** supported on MCM-41 by thermal annealing using electric furnace and oven at 700 °C for 1 hour.

Evaluation for catalytic activity of supported GONP

The liquid phase benzylation of benzene with benzyl chloride (**BzCl**) was selected as a probe reaction for studying the activity of catalysts. The reaction was carried out in a 25 mL round bottomed flask under continuous stirring equipped with condenser, a nitrogen inlet for maintaining an inert atmosphere. The temperature was maintained in oil bath and the reaction carried out at selected reaction condition with reaction temperature of 353 K, benzene to **BzCl** molar ratio of 10, and the catalyst amount of 1 wt% of the total reaction mixture. After 3 hours, the sample was withdrawn and analyzed with ^{1}H NMR measurement. The conversion was based on the consumed in the reaction mixture.

Results and discussion

The **GONP** powder was obtained from **GaNP@DAm** after annealing under air for 1 hour at various temperatures. In the case of annealing temperature above 700 °C, the obtained powder was colourless, while that annealed below 600 °C exhibited gray color. Their crystal phase was identified by XRD, as shown Fig. 2. Whereas the XRD patterns of **GONP** powders treated above 700 °C confirms that most of the strong peaks corresponded with commercial β-Ga_2O_3, powders treated below 600 °C reveal low crystalline nature. This fact indicated the importance of annealing temperature on the crystallinity of **GONP**.

The morphology of products obtained after thermal annealing with various temperatures was investigated by transmission electron microscope (TEM) as shown Fig. 3. It clearly shows nanosized spherical particles treated below 700 °C (Fig. 3b–d), derived from the original **GaNP@DAm** particle

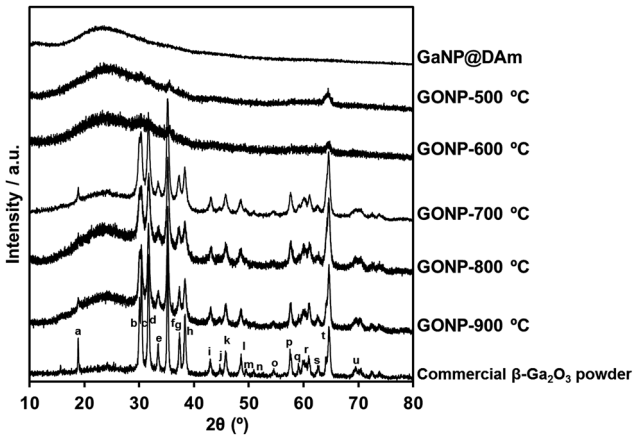

Fig. 2 XRD patterns of the powders annealed with different temperatures of **GaNP@DAm** before annealing, **GONP**-500 °C, **GONP**-600 °C, **GONP**-700 °C, **GONP**-800 °C, **GONP**-900 °C, and commercial β-Ga_2O_3 powder. a: (−201), b: (400), c: (−401), d: (002), (−202), e: (−111), f: (111), g: (401), h: (−311), (−402), (202), i: (−112), j: (−601), k: (600), (−312), (112), l: (510), m: (402), n: (−403), o: (511), (203), p: (−313), q: (113), r: (−801), s: (710), t: (403), (512), (−222), u: (−421), (022), (−222).

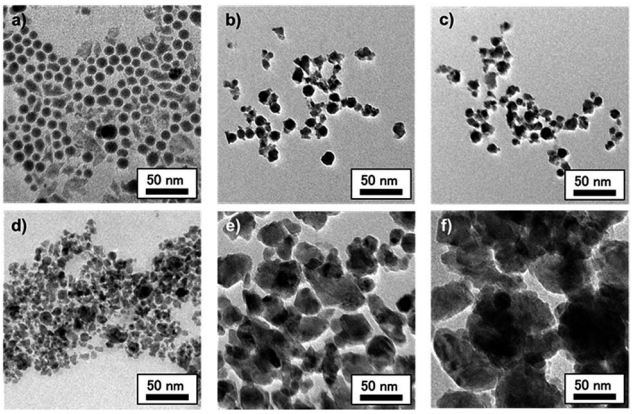

Fig. 3 TEM images of (a) **GaNP@DAm** before annealing, and **GONP** annealed at (b) 500 °C, (c) 600 °C, (d) 700 °C, (e) 800 °C, and (f) 900 °C.

(Fig. 3a). Indeed, the measured particle distribution of **GONP** annealed at 700 °C (15.9 ± 4.2 nm) was similar with that of **GaNP@DAm** (13.3 ± 4.9 nm, Fig. S1†), while the **GONP** partially aggregated to form larger particle (Fig. 3d). With the increase of thermal annealing temperature, the particle was likely to aggregate and formed bulky crystal with irregular morphologies, probably due to due to higher oxidation reaction rate (Fig. 3e and f).

High magnification TEM images of a single particle annealed at various temperatures are shown in Fig. 4a–e. The crystalline nature of these particles was verified by the high-resolution TEM (HRTEM), as shown in Fig. 4f–j. The marked interplanar *d*-spacing of all samples corresponded with facet of β-Ga_2O_3 such as (403), (400) or (111). However for particles treated below 600 °C, the mixed population of crystalline part and amorphous part in a single particle was observed (Fig. 4f and g). Thus, crystallization of **GONP** was completely proceeded above 700 °C.[29]

In order to confirm its single-crystalline character of the particles treated above 700 °C, we obtained selected-area electron diffraction (SAED) pattern from a single particle (Fig. 5). From the SAED patterns of single particle annealed at 700 °C, all the diffraction spots can be indexed to single-crystalline β-Ga_2O_3 (Fig. 5a). On the other hand, the SAED patterns of single particle annealed at 900 °C revealed poly crystalline β-Ga_2O_3 as can be seen in the unindexed spots marked by yellow circle in Fig. 5b.

The result of preparation of **GONP** was summarized in Table 1. These observations offered two facts for preparation of **GONP**. At first, when thermal annealing temperature was 500 °C or 600 °C, crystallization of β-Ga_2O_3 was not completely proceeded with the result that gallium and β-Ga_2O_3 mixed nanoparticles was formed. In the case of thermal annealing temperature above 700 °C, gallium part of **GaNP@DAm** as precursors perfectly transformed into β-Ga_2O_3, resulted in formation of single-crystalline **GONP** at 700 °C. However for the second fact, aggregation and fusion of single-crystalline **GONP** was occurred at 800 °C or 900 °C, which brought about the formation of polycrystalline **GONP**.

Then we focused characteristic and property of single-crystalline **GONP** annealed at 700 °C. We investigated the emission property of the **GONP**. The absorption, excitation, and emission spectra of the **GONP** dispersed in methanol were measured at room temperature, as shown in Fig. 6. The emission spectrum shows a broad light blue emission band centered at 451 nm under a 248 nm excitation. Note that **GONP** prepared at 900 °C exhibited the emission maximum at 470 nm, which was identical to that of commercial β-Ga_2O_3 powder, indicative of the importance of single crystalline nature for the emission property. The band gap (E_g) of **GONP** was estimated by using a Tauc plot of UV-Vis diffuse reflectance spectroscopy (Fig. 6b), which was found to be 4.84 eV. The commercial β-Ga_2O_3 powder showed its band gap at 4.56 eV, thus a quantum size effect of β-Ga_2O_3 caused the 0.28 eV of hypsochromic shift on the band gap, corresponding to the anticipated value from Brus equation (Fig. S2†).[30,31]

The obtained single crystalline **GONP** slightly aggregated due to disappearance of stabilizer through thermal annealing, as shown in Fig. 3d. To suppress aggregation of **GONP** by coating **GaNP** with heat-resistant materials, we attempted to prepare silica coated **GONP** (**GO@SiO_2 NP**) utilizing silica coated **GaNP** (**Ga@SiO_2 NP**) as precursors to suppress aggregation of nanoparticles. Moreover, we selected smaller **GaNP** (**GaNP@OAc**; average diameter: *ca.* 8 nm) compared to **GaNP@DAm** (average diameter: *ca.* 15 nm) as the precursor. **Ga@SiO_2 NP** was obtained through a sol–gel reaction of tetramethyl orthosilicate (TMOS) catalyzed by aqueous ammonia as a catalyst in alcoholic solvent at room temperature. An excess amount of TMOS was employed due to the in stability of **GaNP** in an alcoholic solution. After the sol–gel reaction for 1 hour, **GO@SiO_2 NP** was prepared by thermal annealing at 700 °C for 1 hour. Thermal annealing caused colour change of powder from black to white. Whereas the XRD patterns of

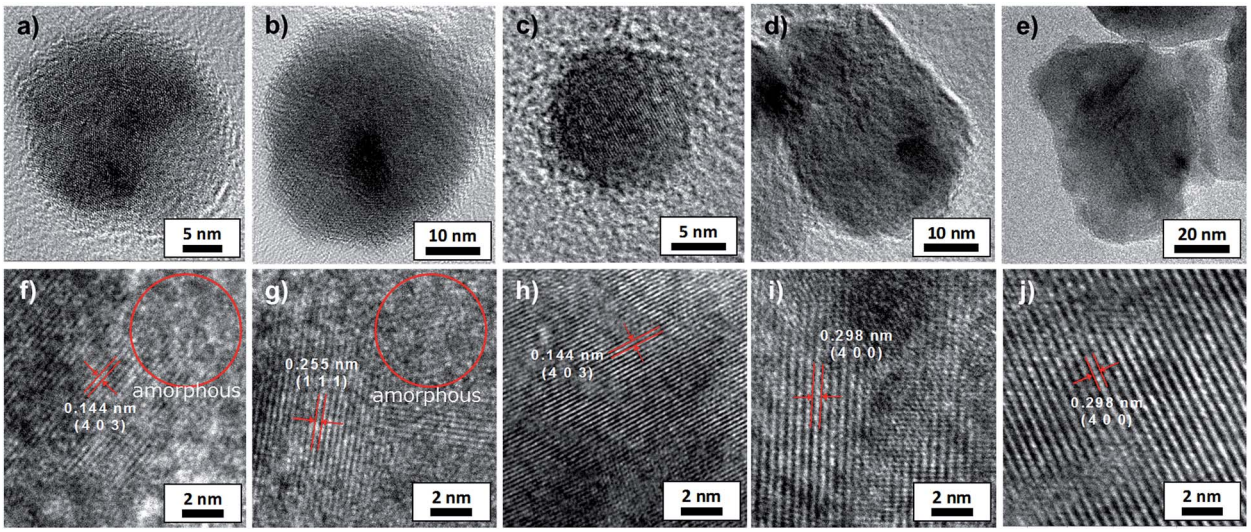

Fig. 4 TEM images of single particle of **GONP** annealed at different temperatures: (a) 500 °C, (b) 600 °C, (c) 700 °C, (d) 800 °C, and (e) 900 °C. HRTEM images of single particle prepared at different temperatures: (f) 500 °C, (g) 600 °C, (h) 700 °C, (i) 800 °C, and (j) 900 °C.

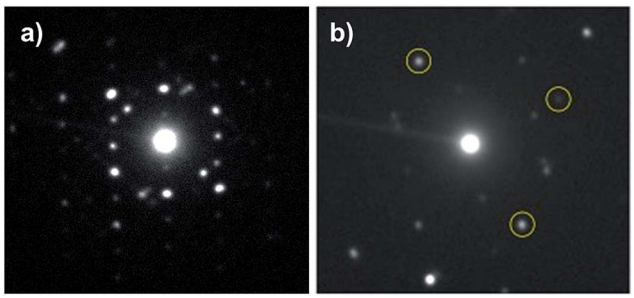

Fig. 5 SAED patterns of single particle of **GONP** annealed at (a) 700 °C, and (b) 900 °C.

Ga@SiO$_2$ NP powder shows amorphous, powders treated at 700 °C confirms weak peaks at 35.3° and 64.3°, respectively attributed to (111) and (403) of β-Ga_2O_3 (Fig. 7).

TEM observation of resulted particles revealed the formation of **GO@SiO$_2$ NP**, which showed similar appearance with **Ga@SiO$_2$ NP** (Fig. 8a and b). The distribution of particle diameter in **GO@SiO$_2$ NP** (9.1 ± 1.6 nm) was close to that of **Ga@SiO$_2$ NP** (9.6 ± 1.8 nm, Fig. S3†). EDX-analysis of **GO@SiO$_2$ NP** proved the existence of Ga and Si atoms as well as those in **Ga@SiO$_2$ NP**. Then we investigated the emission property and bang gap of **GO@SiO$_2$ NP**. Analogous to **GONP**, emission spectrum of **GO@SiO$_2$ NP** showed a broad emission spectrum centered at 446 nm under a 240 nm excitation, which was caused hypsochromic shift compared with **GONP** (Fig. S4†). Furthermore, the band gap of **GO@SiO$_2$ NP** was determined as 4.89 eV from Tauc plot, thus larger than that of **GONP** (Fig. 6b). These results confirmed existence of quantum size effect of β-Ga_2O_3.

To investigate the catalytic activity of **GONP**, benzylation of benzene with benzyl chloride (**BzCl**) has been carried out.[32–34] **GONP/MCM-41** was used for benzylation at the reaction temperature of 80 °C, the reaction time of 3 hours and the benzene to **BzCl** ratio 10 and the results are shown Fig. 9. The major product in the reaction is diphenylmethane (**DPM**). The trace of the formation of by-product (dibenzylbenzene) was found. **BzCl** conversion and **DPM** selectivity were calculated to be 71% and 51%, respectively. The time of frequency (TOF) of this catalysis was found to be 25 h^{-1}. On the other hand, commercial β-Ga_2O_3 powder did not show formation of **DPM** at all. This result revealed that our catalyst was active for the benzylation of benzene with **BzCl**, probably due to the increased surface area of β-Ga_2O_3.

Table 1 The characteristics of **GaNP@DAm** and **GONP** prepared under various condition

Sample	Color	Shape	Composition	Crystallinity
GaNP@DAm	Black	Sphere	Amorphous	—
GONP-500 °C	Gray	Sphere	Amorphous + crystal	—
GONP-600 °C	Gray	Sphere	Amorphous + crystal	—
GONP-700 °C	White	Sphere	Crystal	Single crystal
GONP-800 °C	White	Non-sphere	Crystal	Poly crystal
GONP-900 °C	White	Non-sphere	Crystal	Poly crystal

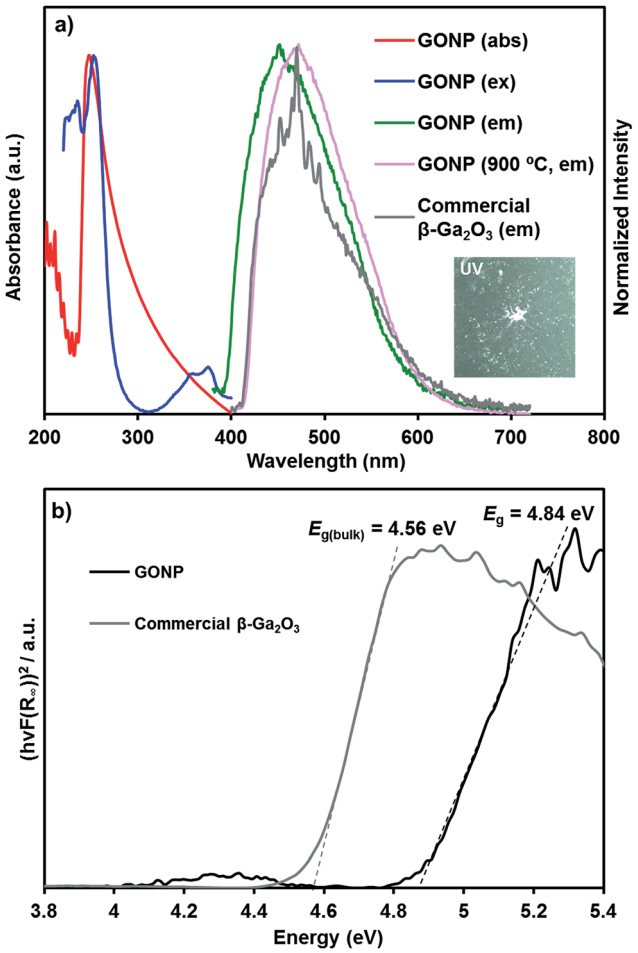

Fig. 6 (a) Absorption, excitation (λ_{em} = 451 nm) and emission spectra (λ_{ex} = 248 nm) of single-crystalline **GONP** and commercial β-Ga_2O_3 powder. Emission spectrum of **GONP** prepared at 900 °C was also shown. Inset shows the photograph of single-crystalline **GONP** under UV irradiation at 254 nm. (b) Band gap data of single-crystalline **GONP** and commercial β-Ga_2O_3 powder obtained from UV reflectance.

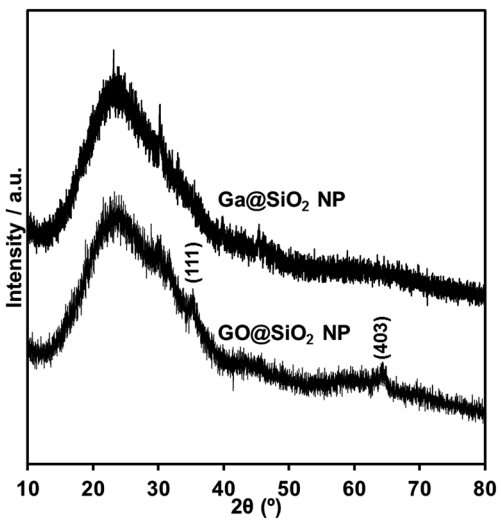

Fig. 7 XRD patterns of silica coated GaNP@OAc (**Ga@SiO_2 NP**) and silica coated **GONP** (**GO@SiO_2 NP**).

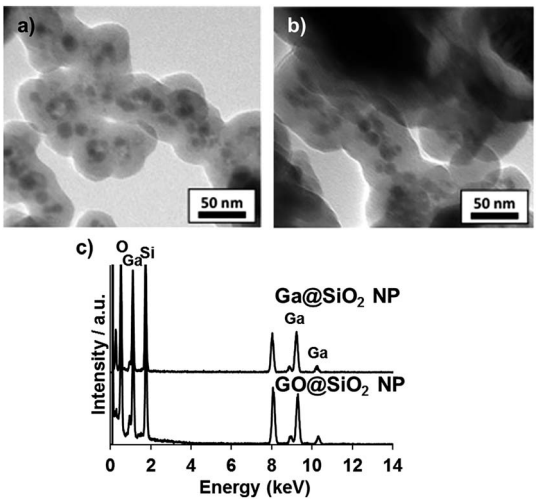

Fig. 8 TEM images of (a) **Ga@SiO_2 NP**, and (b) **GO@SiO_2 NP**, and (c) TEM-EDX analysis of **Ga@SiO_2 NP** and **GO@SiO_2 NP**.

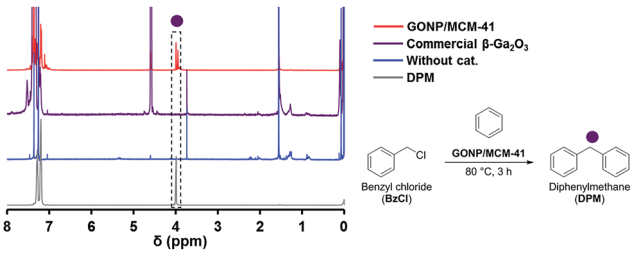

Fig. 9 ^{1}H NMR spectra of sample after benzylation under various conditions.

Conclusions

We have demonstrated a novel approach to prepare nanosized β-Ga_2O_3 particles utilizing **GaNP** as precursors. A strong dependence between the structure of **GONP** and the thermal annealing temperature was observed. Furthermore, it was found that silica coating allowed to maintain the spherical shape of nanoparticles without formation of aggregation and change of morphology (**GO@SiO_2 NP**). The single-crystalline **GONP** with spherical morphology exhibited a light blue emission and band gap shift derived from quantum size effect compared to bulk β-Ga_2O_3. Moreover, MCM-41 supported **GONP** (**GONP/MCM-41**) revealed catalytic activity for benzylation of benzene with **BzCl**. We strongly believe that **GONP** will be suitable for applications in LED phosphors, optoelectronic devices, and supported catalysts.

Acknowledgements

The authors acknowledge financial support from a JSPS Grant-in-Aid for Scientific Research (B) (26288054) and a JSPS Grant-in-Aid for Young Scientists (B) (15K17861). The authors appreciate Prof. M. Kato and Prof. Y. Wang for XRD measurements and TEM (environmental cell) for SAED, respectively. The TEM

observation was carried out at the OPEN FACILITY, Hokkaido University Sousei Hall.

Notes and references

1 H. H. Tippins, *Phys. Rev. [Sect.] A*, 1965, **140**, A316–A319.
2 M. Passlack, E. F. Schubert, W. S. Hobson, M. Hong, N. Moriya, S. N. G. Chu, K. Konstadinis, J. P. Mannaerts, M. L. Schnoes and G. Zydzik, *J. Appl. Phys.*, 1995, **77**, 686–693.
3 K. Yamaguchi, *Solid State Commun.*, 2004, **131**, 739–744.
4 H. He, R. Orlando, M. A. Blanco, R. Pandey, E. Amzallag, I. Baraille and M. Rerat, *Phys. Rev. B: Condens. Matter Mater. Phys.*, 2006, **74**, 195123.
5 M. Passlack, M. Hong and J. P. Mannaerts, *Appl. Phys. Lett.*, 1996, **68**, 1099.
6 Z. Li, C. Groot, J. Jagadeesh and H. Moodera, *Appl. Phys. Lett.*, 2000, **77**, 3630.
7 L. Binet and D. Gourier, *J. Phys. Chem. Solids*, 1998, **59**, 1241–1249.
8 T. Minami, *MRS Bull.*, 2000, **8**, 38–44.
9 M. Ogita, N. Saika, Y. Nakanishi and Y. Hatanaka, *Appl. Surf. Sci.*, 1999, **142**, 188–191.
10 P. Feng, J. Y. Zhang, Q. H. Li and T. H. Wang, *Appl. Phys. Lett.*, 2006, **88**, 153107.
11 X. C. Wu, W. H. Song, W. D. Huang, M. H. Pu, B. Zhao, Y. P. Sun and J. J. Du, *Chem. Phys. Lett.*, 2000, **328**, 5–9.
12 Y. C. Choi, W. S. Kim, Y. S. Park, S. M. Lee, D. J. Bae, Y. H. Lee, G. S. Park, W. B. Choi, N. S. Lee and J. M. Kim, *Adv. Mater.*, 2000, **12**, 746–750.
13 S. Sharma and M. K. Sunkara, *J. Am. Chem. Soc.*, 2002, **124**, 12288–12293.
14 Y. P. Song, H. Z. Zhang, C. Lin, Y. W. Zhu, G. H. Li, F. H. Yang and D. P. Yu, *Phys. Rev. B: Condens. Matter Mater. Phys.*, 2004, **69**, 075304.
15 P. C. Chang, Z. Fan, W. Y. Tseng, A. Rajagopal and J. G. Lu, *Appl. Phys. Lett.*, 2005, **87**, 222102.
16 J. Hu, Q. Li, J. Zhan, Y. Jiao, Z. Liu, S. P. Ringer, Y. Bando and D. Golberg, *ACS Nano*, 2008, **2**, 107–112.
17 Y. Huang, Z. Wang, Q. Wang, C. Gu, C. Tang, Y. Bando and D. Golberg, *J. Phys. Chem. C*, 2009, **113**, 1980–1983.
18 S. Yan, L. Wan, Z. Li, Y. Zhou and Z. Zou, *Chem. Commun.*, 2010, **46**, 6388–6390.
19 J. Lin, Y. Huang, Y. Bando, C. Tang, C. Li and D. Golberg, *ACS Nano*, 2010, **4**, 2452–2458.
20 T. Zhang, J. Lin, X. Zhang, Y. Huang, X. Xu, Y. Xue, J. Zou and C. Tang, *J. Lumin.*, 2013, **140**, 30–37.
21 V. I. Klimov, A. A. Mikhailovsky, S. Xu, A. Malko, J. A. Hollingsworth, C. A. Leatherdale, H. J. Eisler and M. G. Bawendi, *Science*, 2000, **290**, 314–317.
22 A. V. Dijken, E. A. Meulenkamp, D. Vanmaekelbergh and A. Meijerink, *J. Lumin.*, 2000, **90**, 123–128.
23 P. Claus, A. Brückner, C. Mohr and H. Hofmeister, *J. Am. Chem. Soc.*, 2000, **122**, 11430–11439.
24 Y. Volokitin, J. Sinzig, L. J. Jongh, G. Schmid, M. N. Vargaftik and I. I. Moiseev, *Nature*, 1996, **384**, 621–623.
25 R. Viswanatha, S. Sapra, B. Satpati, P. V. Satyam, B. N. Dev and D. D. Sarma, *J. Mater. Chem.*, 2004, **14**, 661–668.
26 C. Lemire, R. Meyer, S. Shaikhutdinov and H. J. Freund, *Angew. Chem., Int. Ed.*, 2004, **43**, 118–121.
27 L. Yin, Y. Wang, G. Pang, Y. Koltypin and A. Gedanken, *J. Colloid Interface Sci.*, 2002, **246**, 78–84.
28 S. Sudo, S. Nagata, K. Kokado and K. Sada, *Chem. Lett.*, 2014, **43**, 1207–1209.
29 S. Penner, B. Klotzer, B. Jenewein, F. Klauser, X. Liu and E. Bertel, *Thin Solid Films*, 2008, **516**, 4742–4749.
30 A. V. Dijken, E. A. Meulenkamp, D. Vanmaekelbergh and A. Meijerink, *J. Lumin.*, 2000, **90**, 123–128.
31 L. Brus, *J. Phys. Chem.*, 1986, **90**, 2555–2560.
32 S. Ajaikumar and A. Pandurangan, *Appl. Catal., A*, 2009, **357**, 184–192.
33 J. Sun, Q. Kan, Z. Li, G. Yu, H. Liu, X. Yang, Q. Huo and J. Guan, *RSC Adv.*, 2014, **4**, 2310–2317.
34 N. Narender, K. V. V. K. Mohan, S. J. Lulkarni and I. A. K. Reddy, *Catal. Commun.*, 2006, **7**, 583–588.